Kinetic Study of the Reaction of Re($a^6S_{5/2}$) with O_2, NO, N_2O, and CH_4

Mark L. Campbell†

Chemistry Department, United States Naval Academy, Annapolis, Maryland 21402

Received: August 7, 1997; In Final Form: October 17, 1997

The gas-phase reactivity of ground-state Re($a^6S_{5/2}$) with O_2, NO, N_2O, and CH_4 is reported. Rhenium atoms were produced by the photodissociation of $Re(CO)_5Cl$ and detected by laser-induced fluorescence. The reaction rate of the $a^6S_{5/2}$ state with O_2 is slow and temperature-dependent. The reaction is pressure-independent, indicating a bimolecular abstraction reaction. The bimolecular rate constant from 296 to 548 K is described in Arrhenius form by $(2.1 \pm 0.3) \times 10^{-11}$ exp(-11.6 ± 0.6 kJ/mol/*RT*) where the uncertainties represent $\pm 2\sigma$. The reaction rate of the $a^6S_{5/2}$ state with NO is pressure-dependent, indicating adduct formation. The limiting low-pressure third-order, k_0, and limiting high-pressure second-order, k_∞, room-temperature rate constants with NO in nitrogen buffer are $(3.7 \pm 0.8) \times 10^{-30}$ cm^6 s^{-1} and $(7.0 \pm 0.8) \times 10^{-12}$ cm^3 s^{-1}, respectively. There is no evidence of chemical reaction for the ground state of rhenium with N_2O or CH_4 up to a temperature of 548 K.

Introduction

The kinetics of the reactions of transition-metal (TM) atoms with oxygen-containing oxidants has recently been an active field of study.[1−41] Gas-phase TM chemistry is an intriguing field of study due to the high multiplicities of the atomic ground states and the large number of low-lying metastable states. The cumulative data reported thus far indicate the electronic state is a very important factor in the dynamics of these reactions. For example, for both the termolecular association and abstraction channels with O_2, TMs with s^1d^{n-1} configurations have been found to be more reactive than their s^2d^{n-2} counterparts.[21,33]

Of the TMs, the 3d and 4d series have garnered the most experimental and theoretical attention[1−13,16−36] while the 5d series remains relatively unstudied. Quite recently, however, studies involving a few of the 5d TMs have been reported.[13−15,37−41] The most complete study of the 5d series has involved reactions with hydrocarbons.[13−15] In the reactions of TMs with hydrocarbons, the 5d series metals are generally more reactive than the 3d metals. This trend has been explained as arising from the better size match between the 6s and 5d orbitals relative to the 4s and 3d orbitals of the 3d series.[14] This better size match helps drive the chemical reaction due to the increased bond energy of the metal−carbon or metal−hydrogen bonds in the product. For reactions with oxygen-containing molecules, the 5d series again appears to be more reactive than the 3d series although this trend is based on only a few 5d metals.[37−41] More experimental studies are required to substantiate this trend.

In this paper we report a temperature- and pressure-dependent kinetic study of the $6s^25d^5$ $a^6S_{5/2}$ state of rhenium with oxygen, nitric oxide, nitrous oxide, and methane. We also report room-temperature removal rate constants for the two lowest lying excited electronic states. Rhenium is unusual among the TMs due to its relatively isolated $6s^25d^5$ ground-state configuration; i.e., the lowest excited state is 11 584 cm^{-1} above the ground state.[42] We are unaware of any previous kinetics studies for gas-phase rhenium. The reporting of these reactions for rhenium will further update the database of TM reactions and allow comparison of rhenium's kinetic behavior with other TMs. Unfortunately, theoretical calculations involving the 5d series are extremely difficult due to the complications arising from electron correlation, relativistic, and spin−orbit effects. Moderately successful theoretical studies involving platinum and iridium with methane have been reported.[14] We hope these new kinetic results will inspire further theoretical work in an effort to further understand these reactions.

Experimental Section

Pseudo-first-order kinetic experiments ([Re] ≪ [oxidant]) were carried out in an apparatus with slowly flowing gas using a laser photolysis/laser-induced fluorescence (LIF) technique. The experimental apparatus and technique have been described in detail elsewhere.[37] Briefly, the reaction chamber is a stainless steel reducing four-way cross with attached sidearms and a sapphire window for optical viewing. The reaction chamber is enclosed within a convection oven (Blue M, model 206F) for temperature dependence experiments.

Rhenium atoms were produced by the 248 nm photodissociation of rhenium pentacarbonyl chloride [$Re(CO)_5Cl$] using the output of an excimer laser (Lambda Physics Lextra 200). Rhenium atoms were detected via LIF using an excimer-pumped dye laser (Lambda Physics Lextra 50/ScanMate 2E) tuned to the $z^6P_{7/2}^\circ \leftarrow a^6S_{5/2}$ transition at 346.046 nm.[43] A few experiments utilized the $z^6P_{3/2}^\circ \leftarrow a^6S_{5/2}$ transition at 345.188 nm, the $z^6D_{5/2}^\circ \leftarrow a^6S_{5/2}$ transition at 299.236 nm, and the $z^8P_{7/2}^\circ \leftarrow a^6S_{5/2}$ transition at 488.914 nm. Experimental results were found to be independent of the optical transition employed. The fluorescence was detected at 90° to the counterpropagated laser beams with a three-lens telescope imaged through an iris. A photomultiplier tube (Hamamatsu R375) was used in collecting the LIF which was subsequently sent to a gated boxcar sampling module (Stanford Research Systems SR250), and the digitized output was stored and analyzed by a computer. The primary focus of this study was on the $a^6S_{5/2}$ ground state; however, the

† Henry Dreyfus Teacher−Scholar.

S1089-5639(97)02584-X This article not subject to U.S. Copyright. Published 1998 by the American Chemical Society
Published on Web 01/14/1998

two lowest excited states, $a^4P_{5/2}$ (11 584 cm^{-1}) and $a^6D_{9/2}$ (11 755 cm^{-1}), were also studied at room temperature to determine the effect of excited-state relaxation on the temporal profiles of the ground state. The transitions used to observe these states were the $y^6D_{7/2}^\circ \leftarrow a^4P_{5/2}$ transition at 340.472 nm and the $y^6D_{7/2}^\circ \leftarrow a^6D_{9/2}$ transition at 342.462 nm.[43] For the study of the excited states, the photolysis laser output was focused using a lens ($f = 564$ mm) positioned approximately one focal length from the detection zone. The focused excimer produced a much stronger signal of excited-state atoms than the unfocused beam.

The rhenium precursor was entrained in a flow of buffer gas. The precursor carrier gas, buffer gas, and reactant gases flowed through calibrated mass flow meters and flow controllers prior to admission to the reaction chamber. Each sidearm window was purged with a slow flow of buffer gas to prevent deposition of rhenium and other photoproducts. Total flows were between 250 and 2800 sccm, although most experiments had flows of approximately 600 sccm. Pressures were measured with MKS Baratron manometers, and chamber temperatures were measured with a thermocouple.

The delay time between the photolysis pulse and the dye-laser pulse was varied by a digital delay generator (Stanford Research Systems DG535) controlled by a computer. The trigger source for these experiments was scattered pump laser light incident upon a fast photodiode. LIF decay traces consisted of 200 points, each point averaged for four laser shots.

Materials. Rhenium pentacarbonyl chloride (Strem, 98%), O_2 (MG Industries, 99.8%), N_2O (MG Industries, electronic grade, 99.999%), CH_4 (Linde, ultrahigh purity grade, 99.99%), N_2 (Potomac Airgas, Inc., 99.998%), and He (Air Products, 99.998%) were used as received. The NO (Liquid Carbonic, 99%) was passed through a liquid nitrogen/*n*-pentane trap at approximately −100 °C to condense impurities (primarily NO_2) before entrance into the reaction chamber.

Data Analysis and Results

The decay rates of the ground state ($a^6S_{5/2}$) of rhenium as a function of reactant pressure were investigated in N_2 buffer gas at various temperatures and total pressures. The loss of ground-state rhenium is described by the first-order decay constant, k_1:

$$k_1 = 1/\tau = k_o + k_2[\text{oxid}] \qquad (1)$$

where τ is the first-order time constant for the removal of rhenium under the given experimental conditions, k_o is the loss term due to diffusion out of the detection zone and reaction with the precursor and precursor fragments, and k_2 is the second-order rate constant. Typical decay profiles are shown in Figure 1. A time constant, τ, for each decay profile was determined using a linear least-squares procedure. The second-order rate constant is determined from a plot of $1/\tau$ vs reactant number density. Typical plots for obtaining second-order rate constants are presented in Figures 2 and 3; the slope yields the observed rate constant. The relative uncertainty (i.e., the reproducibility) of the second-order rate constants is estimated at ±20% based on repeated measurements of rate constants under identical temperature and total pressure conditions. The absolute uncertainties are conservatively estimated to be ±40% and are based on the sum of the statistical scatter in the data, uncertainty in the flowmeter and flow controller readings (5%) and the total pressure reading (1%), and uncertainties due to incomplete gas mixing.

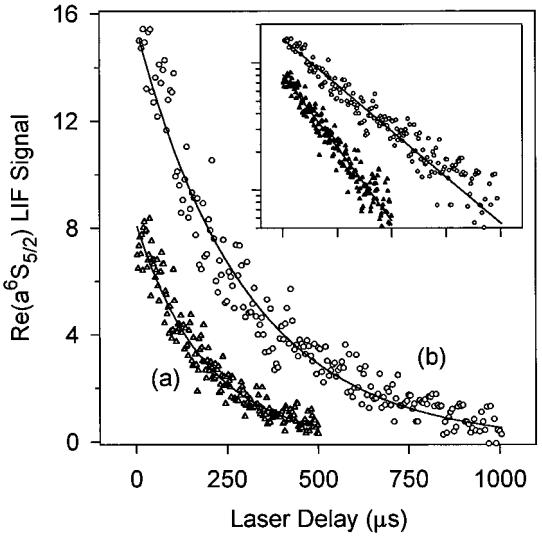

Figure 1. Typical Re($a^6S_{5/2}$) decay curves with added oxidant in N_2 buffer ($T = 296$ K, $P_{total} = 20.0$ Torr): (a) $P(NO) = 0.078$ Torr, $\tau = 185$ μs; (b) $P(O_2) = 0.57$ Torr, $\tau = 300$ μs. The solid lines through the data are exponential fits. The inset is a ln plot of the data.

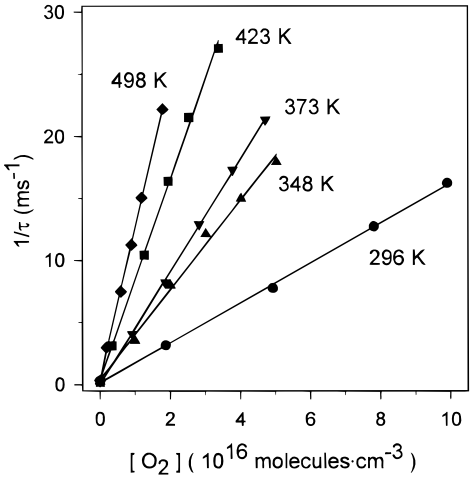

Figure 2. Typical plots for determining k_{2nd} for Re($a^6S_{5/2}$) + O_2 illustrating the dependence of the bimolecular rate constants on temperature. The solid line for each set of data is a linear regression fit from which k_{2nd} is obtained.

Measured rate constants for the $a^6S_{5/2}$ state reacting with O_2 at 20 Torr total pressure from 296 to 548 are listed in Table 1. Rate constants could not be measured above 548 K due to thermal decomposition of the precursor. The rate constants at 296 K for this reaction were measured at 10, 20, 50, and 100 Torr and are independent of total pressure within experimental uncertainty. An Arrhenius plot of the rate constants is shown in Figure 4. The rate constants are described by

$$k(T) = (2.1 \pm 0.3) \times 10^{-11} \exp(-11.6 \pm 0.6 \text{ kJ/mol}/RT) \qquad (2)$$

where the uncertainties are $\pm 2\sigma$.

Measured rate constants for the $a^6S_{5/2}$ state reacting with NO in nitrogen buffer at various pressures are listed in Table 2. The second-order rate constant was also measured at 373 K and 20 Torr and determined to be 1.7×10^{-12} cm^3 s^{-1}. Thus, the rate constants are dependent on total pressure and decrease with increasing temperature, indicating a termolecular process. The variation with total pressure of the second-order rate constants at room temperature in N_2 buffer are shown in Figure

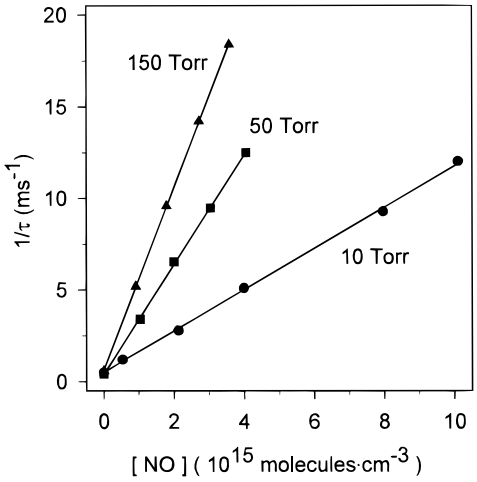

Figure 3. Typical plots for determining k_{2nd} for Re($a^6S_{5/2}$) + NO, indicating the dependence of the second-order rate constants on total pressure. The solid line for each set of data is a linear regression fit from which k_{2nd} is obtained.

TABLE 1: Second-Order Rate Constants for Re($a^6S_{5/2}$) + O_2 at 20 Torr

temp (K)	k_{2nd} (10^{-13} cm^3 s^{-1})	temp (K)	k_{2nd} (10^{-13} cm^3 s^{-1})
296	1.8	448	9.4
348	3.6	473	11
373	5.0	498	12
398	6.5	523	15
423	8.0	548	16

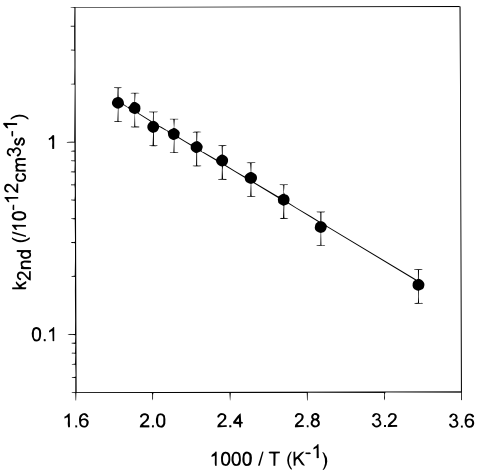

Figure 4. Arrhenius plot for the collisional disappearance of Re($a^6S_{5/2}$) with O_2. Error bars represent ±20% uncertainty.

TABLE 2: Second-Order Rate Constants for Re($a^6S_{5/2}$) + NO in N_2 Buffer at 296 K

total press. (Torr)	k_{2nd} (10^{-12} cm^3 s^{-1})	total press. (Torr)	k_{2nd} (10^{-12} cm^3 s^{-1})
5	0.69	75	3.8
10	1.1	100	4.2
20	2.1	150	5.0
50	3.1	200	5.7

5. The solid lines through the data in Figure 5 are weighted fits to the simplified Lindemann−Hinshelwood expression[44]

$$k = \frac{k_0[\mathrm{M}]}{1 + k_0[\mathrm{M}]/k_\infty} \qquad (3)$$

where k_0 is the limiting low-pressure third-order rate constant,

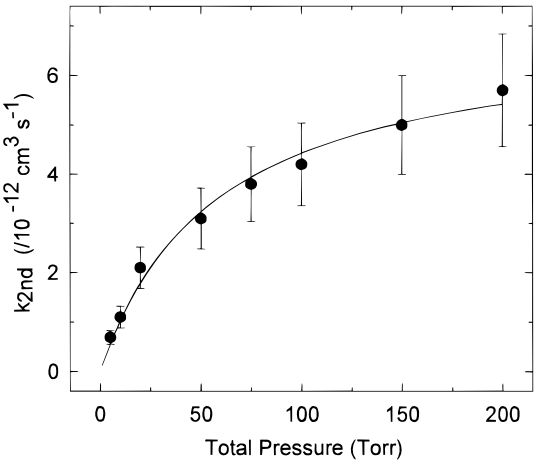

Figure 5. Pressure dependence of the reaction of Re($a^6S_{5/2}$) with NO in N_2 buffer at room temperature. Error bars represent ±20% uncertainty. The solid lines are fits to eq 3.

TABLE 3: Removal Rate Constants (10^{-11} cm^3 s^{-1}) for the $a^4P_{5/2}$ and $a^6D_{9/2}$ States of Rhenium in He Buffer at 296 K and 20 Torr

	N_2	O_2	NO	N_2O	CH_4
$a^4P_{5/2}$	0.61	8.8	13	5.1	0.0013
$a^6D_{9/2}$	0.53	7.7	13	4.8	0.0025

k_∞ is the limiting high-pressure second-order rate constant, and [M] is the buffer gas number density. The values for k_o and k_∞ for the reaction of NO in N_2 buffer at room temperature are $(3.7 \pm 0.8) \times 10^{-30}$ cm^6 s^{-1} and $(7.0 \pm 0.8) \times 10^{-12}$ cm^3 s^{-1}, respectively. The listed uncertainties are $\pm 2\sigma$.

For the reactions of ground-state rhenium with N_2O and CH_4, there is no indication of chemical removal up to a temperature of 548 K. Under the experimental conditions employed in this study, the sensitivity (lower limit) of our apparatus is 1×10^{-15} cm^3 s^{-1}. Thus, the reactions of Re($a^6S_{5/2}$) with N_2O and CH_4 have rate constants of 1×10^{-15} cm^3 s^{-1} or less at temperatures of 548 K and lower.

The decay rates of the two lowest excited states of rhenium, $a^4P_{5/2}$ and $a^6D_{9/2}$, as a function of reactant pressure were investigated in He buffer gas at room temperature and 20 Torr pressure. These states could not be studied in N_2 buffer due to the efficient quenching of these states by this gas. The decay profiles showed growth (i.e., nonexponential behavior) at the beginning of the decay profiles. We attribute this behavior to the relaxation of higher electronically excited states to these lowest lying metastable states. Time constants were determined by adjusting the range of the linear regression analysis; i.e., the range did not include the beginning of the decay when growth was present. Decays were typically analyzed after a delay of up to one reaction lifetime and included data for a length of two to three reaction lifetimes. The measured rate constants are tabulated in Table 3. The uncertainty of these second-order rate constants are estimated at ±50%. The larger errors relative to the ground-state rate constants are due to the difficulty in accurately fitting the decay profiles with growth. The rate constants of the excited states are all at least an order of magnitude greater than the rate constants of the ground state. Furthermore, the relatively large removal rate constants of these two states interacting with N_2 indicate these excited states are short-lived in moderately high pressures of N_2. Thus, the lowest lying excited states do not affect the decay profiles of the ground state.

TABLE 4: Enthalpies[45−47] of Reaction and Arrhenius Parameters for the Transition-Metal Atom Reaction TM(g) + O_2(g) → TMO(g) + O(g)

TM	$\Delta H°$ (kJ/mol)	E_a (kJ/mol)	A (10^{-10} cm^3 s^{-1})	ref
Sc(s^2d^1 ^{2}D)	−183	7.9	1.7	34
Ti(s^2d^2 ^{3}F)	−170	11.6	1.7	24
V(s^2d^3 ^{4}F)	−139	9.0	1.2	23
Nb(s^1d^4 ^{6}D)	−285	0	2.5	33
Mo(s^1d^5 ^{7}S)	−99	0	1.0	28
Ta(s^2d^3 ^{4}F)	−340	7.8	1.7	40
W(s^2d^4 ^{5}D)	−177	12.7	2.5	37
Re(s^2d^5 ^{6}S)	−124	11.6	0.21	this work
Os(s^2d^6 ^{5}D)	−57	9.0	0.27	39

Discussion

Re + O_2. Results for the reaction of rhenium with O_2 indicate a bimolecular abstraction reaction mechanism:

$$\mathrm{Re}(a^6S_{5/2}) + O_2 \rightarrow \mathrm{ReO} + \mathrm{O} \qquad (4)$$

This reaction is exothermic by approximately 125 kJ/mol;[45−47] thus, there are no thermodynamic barriers to this reaction. Since the reaction proceeds via an O atom abstraction, the energy barrier is expected to arise from the interaction between two surfaces, i.e., a crossing or an avoided crossing. Thus, it is expected that the barrier height might correlate to the difference in the asymptotic energies of these surfaces. Since the ground state of rhenium is relatively isolated, it is not surprising that its room-temperature rate constant is the smallest of all the exothermic reactions of TMs with O_2 while its activation energy is one of the largest. Table 4 tabulates the experimentally measured Arrhenius parameters for TMs with exothermic reactions with O_2. A comparison of the activation energies of these reactions indicates the activation energy of rhenium is similar to other s^2d^{n-2} atoms proceeding by a bimolecular abstraction mechanism.

The reactions of Sc, Ti, and V with O_2 have been studied by us[24,34] and others.[17,18,23,25] Each of these atoms has an s^2d^{n-2} ground-state electron configuration, and termolecular processes for these metals with O_2 are unimportant. In each case the abstraction channel has a barrier of about 10 kJ/mol. Studies of the excited states of vanadium[23] and titanium[25] indicate the excited s^1d^{n-1} states in the presence of O_2 have removal rate constants over an order of magnitude greater than the ground s^2d^{n-2} states. The reactions of the group 6 metals tungsten[37] and molybdenum[28] show similar behavior with O_2 in its bimolecular abstraction reactive channel. In both cases, the s^1d^5 a^7S_3 state is more reactive than the s^2d^4 a^5D_J states. This observation was particularly surprising for Mo since the s^2d^4 states have over 10 000 cm^{-1} more energy than the ground s^1d^5 a^7S_3 state. In tungsten, the s^1d^5 a^7S_3 state was much more reactive than the s^2d^4 a^5D_J states even though the a^5D_2, a^5D_3, and a^5D_4 states have more electronic energy.

A similar result in which the excited s^2d^{n-2} states are less reactive than the lower energy s^1d^{n-1} states has been observed for niobium. The ground state of niobium ($5s^14d^4$ $a^6D_{1/2}$) and the spin−orbit excited states of the ground term react near the gas kinetic collision rate with O_2, while the $5s^24d^3$ $^4F_{9/2}$ state with 2805 cm^{-1} more electronic energy than the ground-state reacts about 50 times slower at room temperature.[33]

The two transition metals with s^1d^{n-1} ground-state configurations (Nb and Mo) exhibit no barrier to reaction with O_2. Thus, for the reaction of gas-phase transition-metal atoms with O_2, the same relationship appears to operate with the bimolecular abstraction mechanism as with the termolecular process;[21] i.e., transition metals with s^1d^{n-1} ground-state configurations react more efficiently than transition metals with s^2d^{n-2} configurations. Unfortunately, a more thorough quantitative understanding of the dynamics of these reactions will have to await more accurate theoretical calculations.

TABLE 5: Termolecular Modeling Parameters for the Reactions of Re(^{6}S), Cr(^{7}S), Mn(^{6}S), Fe(^{5}D), Mo(^{7}S), and Ru(^{5}F) with NO at Room Temperature

TM	k_0 (cm^6 s^{-1})	k_∞ (cm^3 s^{-1})	ref
Cr (Ar)	$(1.2 \pm 0.2) \times 10^{-30}$	$(3.2 \pm 0.8) \times 10^{-11}$	20
Mn (Ar)	$(3.9 \pm 0.6) \times 10^{-33}$	$\sim 3 \times 10^{-13}$	36
Fe (N_2)	$(2.3 \pm 0.3) \times 10^{-32}$	$\sim 5 \times 10^{-13}$	36
Fe (Ar)	$(1.5 \pm 0.2) \times 10^{-32}$	$\sim 8 \times 10^{-13}$	36
Mo (Ar)	$(2.6 \pm 0.3) \times 10^{-29}$	$(5.8 \pm 0.5) \times 10^{-11}$	31
Ru (Ar)	$(8.0 \pm 0.8) \times 10^{-30}$	$(5.4 \pm 4.9) \times 10^{-11}$	36
Ru (N_2)	$(7.3 \pm 1.5) \times 10^{-30}$	5.4×10^{-11}(fixed)	36
Re (N_2)	$(3.7 \pm 0.8) \times 10^{-30}$	$(7.0 \pm 0.8) \times 10^{-12}$	this work

Re + NO. Results of the reaction of Re($a^6S_{5/2}$) + NO indicate a termolecular reaction mechanism. Production of ReO from this reaction is not thermodynamically favorable at 296 K as the abstraction reaction is endothermic.[45−47] Termolecular processes are expected for the majority of the TMs reacting with NO since only the group 3, 4, and 5 atoms along with tungsten have exothermic reactions for the abstraction channel. Thus far, however, extensive pressure-dependent rate constants have only been reported for chromium,[20] iron,[36] manganese,[36] molybdenum,[31] and ruthenium.[36] Table 5 tabulates the third-order parameters for these reactions. The two atoms in the 3d series with s^2d^{n-2} electron configurations are extremely inefficient whereas the TMs with s^1d^{n-1} configurations have much more efficient processes. In the s^1 configuration, the singly occupied orbital of the TM might overlap favorably with the unpaired electron on NO, forming a bond. This argument has been used to explain the reactivity dependence on electron configuration in the termolecular reactions of 3d TM atoms with O_2.[21] Even if the d electrons of the TM atom are involved in the bonding, the reactivity of the s^2 configuration would still be expected to be less than that of the s^1 configuration because of its more diffuse nature.

The termolecular parameters for rhenium are considerably larger than the parameters of the other s^2d^{n-2} TM atoms listed in Table 5. In fact, the rhenium parameters are on the same order of magnitude as those parameters of the s^1d^{n-1} TM atoms. The much higher efficiency of this reactions may be due to the better size match between the 6s and 5d orbitals compared to the 4s and 3d orbitals of the 3d series. The better size match might help drive the chemical reaction due to the increased incorporation of the d orbitals in the bonding to yield larger metal−oxygen bond energies in the product. Again, a more thorough quantitative understanding of the dynamics of this reaction awaits more accurate theoretical calculations.

Re + N_2O. Results for the reaction of rhenium with N_2O indicate a very inefficient process. Abstraction reactions of all TM atoms with N_2O are exothermic due to the formation of the stable N_2 and metal oxide molecules. Despite this exothermicity, metal atom reactions with N_2O have been observed to have significant energy barriers. These barriers have been attributed to the requirement of a nonadiabatic transition along the reaction pathway.[48]

For rhenium reacting with N_2O to produce ReO, the abstraction reaction is exothermic by 244 kJ/mol.[45−47] Experimentally, we were unable to detect a bimolecular component for this reaction up to a temperature of 548 K. Assuming a maximum value of 1×10^{-15} cm^3 s^{-1} for the second-order rate constant for the abstraction channel at 548 K and assuming a preexponential factor of 5×10^{-11} cm^3 s^{-1}, an estimate of the minimum

activation energy for this reaction is calculated to be approximately 50 kJ/mol. This minimum barrier is only slightly greater than the experimentally measured activation energy for the abstraction reaction of $4s^23d^5\ a^6S_{5/2}$ Mn with N_2O ($E_a = 45$ kJ/mol).[30]

Recently, Fontijn and co-workers have advanced a resonance interaction model[49−52] to predict barriers to reaction and rate constants for metal atoms reacting with N_2O. In this model, the activation barriers are calculated by taking into account the ionization potential and sp promotion energy of the metal, the electron affinity of N_2O, and the bond energy of the metal oxide product. The resonance interaction model predicts the energy barrier for the reaction of rhenium with N_2O to be 20 kJ/mol,[49] a value considerably smaller than our lower estimate.

Re + CH_4. The two most plausible reaction pathways for the reaction of rhenium with methane are the termolecular insertion channel to produce $H-Re-CH_3$ and the bimolecular H_2 elimination reaction to produce $Re-CH_2$. Both reaction channels are expected to have very large barriers based on calculations;[53] thus, it is not surprising that a reactive channel was not observed in this study for this reaction.

Summary

We have measured the rate constants as a function of temperature and pressure for the reaction of ground-state rhenium ($a^6S_{5/2}$) with O_2, NO, N_2O, and CH_4. The reaction of rhenium with O_2 is consistent with a bimolecular abstraction reaction. The reaction is slow with an activation energy of 11.6 kJ/mol. The reaction of ground-state rhenium with NO involves a termolecular process. For NO, the reaction is rapid compared to other termolecular reactions involving s^2d^{n-2} transition metals. For the reactions of rhenium with N_2O and CH_4, there is no indication of chemical removal of the ground state up to a temperature of 548 K.

Acknowledgment. This research was supported by a Cottrell College Science Award of Research Corporation. Acknowledgment is made to the donors of the Petroleum Research Fund, administered by the American Chemical Society, for partial support of this research.

References and Notes

(1) Ritter, D.; Weisshaar, J. C. *J. Am. Chem. Soc*. **1990**, *112*, 6425.
(2) Ritter, D.; Carroll, J. J.; Weisshaar, J. C. *J. Phys. Chem*. **1992**, *96*, 10636.
(3) Blomberg, M. R. A.; Siegbahn, P. E. M.; Nagashima, U.; Wennerberg, J. *J. Am. Chem. Soc*. **1991**, *113*, 424.
(4) Carroll, J. J.; Weisshaar, J. C. *J. Am. Chem. Soc*. **1993**, *115*, 800.
(5) Carroll, J. J.; Haug, K. L.; Weisshaar, J. C. *J. Am. Chem. Soc*. **1993**, *115*, 6962.
(6) Carroll, J. J.; Haug, K. L.; Weisshaar, J. C.; Blomberg, M. R. A.; Siegbahn, P. E. M.; Svensson, M. *J. Phys. Chem*. **1995**, *99*, 13955.
(7) Wen, Y.; Yethiraj, A.; Weisshaar, J. C. *J. Chem. Phys*. **1997**, *106*, 5509.
(8) Blitz, M. A.; Mitchell, S. A.; Hackett, P. A. *J. Phys. Chem*. **1991**, *95*, 8719.
(9) Brown, C. E.; Mitchell, S. A.; Hackett, P. A. *Chem. Phys. Lett*. **1992**, *191*, 175.
(10) Lian, L.; Mitchell, S. A.; Rayner, D. M. *J. Phys. Chem*. **1994**, *98*, 11637.
(11) Senba, K.; Matsui, R.; Honma, K. *J. Phys. Chem*. **1995**, *99*, 13992.
(12) Campbell, M. L. *J. Am. Chem. Soc*. **1997**, *119*, 5984.
(13) Parnis, J. M.; Lafleur, R. D.; Rayner, D. M. *J. Phys. Chem*. **1995**, *99*, 673.
(14) Carroll, J. J.; Weisshaar, J. C.; Siegbahn, P. E. M.; Wittborn, C. A. M.; Blomberg, M. R. A. *J. Phys. Chem*. **1995**, *99*, 14388.
(15) Carroll, J. J.; Weisshaar, J. C. *J. Phys. Chem*. **1996**, *100*, 12355.
(16) Vinckier, C.; Corthouts, J.; DeJaegere, S. J. *Chem. Soc., Faraday Trans. 2* **1988**, *84*, 1951.
(17) Ritter, D.; Weisshaar, J. C. *J. Phys. Chem*. **1989**, *93*, 1576.
(18) Ritter, D.; Weisshaar, J. C. *J. Phys. Chem*. **1990**, *94*, 4907.
(19) Mitchell, S. A.; Hackett, P. A. *J. Chem. Phys*. **1990**, *93*, 7822.
(20) Parnis, J. M.; Mitchell, S. A.; Hackett, P. A. *J. Phys. Chem*. **1990**, *94*, 8152.
(21) Brown, C. E.; Mitchell, S. A.; Hackett, P. A. *J. Phys. Chem*. **1991**, *95*, 1062.
(22) Narayan, A. S.; Futerko, P. M.; Fontijn, A. *J. Phys. Chem*. **1992**, *96*, 290.
(23) McClean, R. E.; Pasternack, L. *J. Phys. Chem*. **1992**, *96*, 9828.
(24) Campbell, M. L.; McClean, R. E. *J. Phys. Chem*. **1993**, *97*, 7942.
(25) Clemmer, D. E.; Honma, K.; Koyano, I. *J. Phys. Chem*. **1993**, *97*, 11480.
(26) Helmer, M.; Plane, J. M. C. *J. Chem. Soc., Faraday Trans*. **1994**, *90*, 395.
(27) Fontijn, A.; Blue, A. S.; Narayan, A. S.; Bajaj, P. N. *Combust. Sci. Technol*. **1994**, *101*, 59.
(28) Campbell, M. L.; McClean, R. E.; Harter, J. S. S. *Chem. Phys. Lett*. **1995**, *235*, 497.
(29) Campbell, M. L.; Metzger, J. R. *Chem. Phys. Lett*. **1996**, *253*, 158.
(30) Campbell, M. L. *J. Chem. Phys*. **1996**, *104*, 7515.
(31) McClean, R. E.; Campbell, M. L.; Goodwin, R. H. *J. Phys. Chem*. **1996**, *100*, 7502.
(32) Campbell, M. L. *J. Chem. Soc., Faraday Trans*. **1996**, *92*, 4377.
(33) McClean, R. E.; Campbell, M. L.; Kölsch, E. J. *J. Phys. Chem. A* **1997**, *101*, 3348.
(34) Campbell, M. L.; Hooper, K. L.; Kölsch, E. J. *Chem. Phys. Lett*. **1997**, *274*, 7.
(35) Matsui, R.; Senba, K.; Honma, K. *J. Phys. Chem. A* **1997**, *101*, 179.
(36) McClean, R. E.; Campbell, M. L.; Vorce, M. D. Manuscript in preparation.
(37) Campbell, M. L.; McClean, R. E. *J. Chem. Soc., Faraday Trans*. **1995**, *91*, 3787.
(38) Harter, J. S. S.; Campbell, M. L.; McClean, R. E. *Int. J. Chem. Kinet*. **1997**, *29*, 367.
(39) Campbell, M. L. *J. Phys. Chem*. **1996**, *100*, 19430.
(40) Campbell, M. L.; Hooper, K. L. *J. Chem. Soc., Faraday Trans*. **1997**, *93*, 2139.
(41) Campbell, M. L. *J. Phys. Chem. A* **1997**, *101*, 9377.
(42) Moore, C. E. *NBS Circular 467*; U.S. Department of Commerce: Washington, DC, 1971; Vol. III.
(43) Meggers, W. F.; Corliss, C. H.; Scribner, B. F. *Tables of Spectral-Line Intensities, Part I Arranged by Elements*; NBS Monograph 145; U.S. Government Printing Office: Washington, DC, 1975.
(44) Robinson, P. J.; Holbrook, K. A. *Unimolecular Reactions*; Wiley-Interscience: New York, 1972.
(45) Wagman, D. D.; Evans, W. H.; Parker, V. B.; Schumm, R. H.; Halow, I.; Bailey, S. M.; Churney, K. L.; Nuttall, R. L. The NBS tables of chemical thermodynamic properties; *J. Phys. Chem. Ref. Data* **1982**, *11* (Suppl. 2).
(46) Pedley, J. B.; Marshall, E. M. *J. Phys. Chem. Ref. Data* **1983**, *12*, 967.
(47) Chase, Jr., M. W.; Davies, C. A.; Downey, Jr., J. R.; Frurip, D. J.; McDonald, R. A.; Syverud, A. N. *J. Phys. Chem. Ref. Data* **1985**, *14* (Suppl. 1).
(48) Jonah, C. D.; Zare, R. N.; Ottinger, C. J. *J. Chem. Phys*. **1972**, *56*, 263.
(49) Futerko, P. M.; Fontijn, A. *J. Chem. Phys*. **1991**, *95*, 8065.
(50) Futerko, P. M.; Fontijn, A. *J. Chem. Phys*. **1992**, *97*, 3861.
(51) Futerko, P. M.; Fontijn, A. *J. Chem. Phys*. **1993**, **98**, 7004.
(52) Belyung, D. P.; Futerko, P. M.; Fontijn, A. *J. Chem. Phys*. **1995**, *102*, 155.
(53) Wittborn, A. M.; Costas, M.; Blomberg, M. R. A.; Siegbahn, P. E. M. *J. Chem. Phys*. **1997**, *107*, 4318.